Regional and Temporal Variability of Atmospheric Conditions along the Meiyu-Baiu Front

Sicheng He[1,2] and Tetsuya Takemi[1]

[1]*Disaster Prevention Research Institute, Kyoto University, Uji, Kyoto, Japan*
[2]*Graduate School of Science, Kyoto University, Kyoto, Japan*

(Manuscript received 19 September 2024, accepted 26 February 2025)

Abstract East Asia experiences a distinctive summer rainfall period, referred to as Meiyu in China and Baiu in Japan. The precipitation during the Meiyu-Baiu season is a critical component of summer rainfall, significantly impacting agriculture and economic development. While both Southeast China (SEC) and Japan (JPN) encounter the Meiyu-Baiu season from June to July, the structure of the Meiyu-Baiu front (MBF) differs between these regions. Utilizing daily ERA5 reanalysis data and a method that defines the MBF based on equivalent potential temperature, we analyzed precipitation patterns and atmospheric conditions during the East Asian monsoon season. The MBF demonstrates a distinct northward progression in SEC from early June to late July, whereas in JPN, the front moves northward from early June to mid-July, stagnating thereafter. Meiyu-Baiu precipitation correlates strongly with the position of the MBF during early June to mid-July, with two major precipitation centers identified in both SEC and JPN. Atmospheric conditions associated with the MBF exhibit clear regional and temporal variability. Compared to JPN, SEC features a stronger meridional humidity gradient, more pronounced upward motion, and a smaller meridional temperature gradient on the southern side of the MBF.

Citation: He, S., and T. Takemi, 2025: Regional and temporal variability of atmospheric conditions along the Meiyu-Baiu front. *SOLA*, **21**, 151−157, doi:10.2151/sola.2025-019.

1. Introduction

The Meiyu (China) and Baiu (Japan) seasons are distinctive rainy periods occurring during the late spring to early summer, marking the progression of the East Asian summer monsoon (e.g., Tao and Chen 1987; Ding 1992; Ding et al. 2007). The rainfall during the Meiyu-Baiu season can last from several days to a few weeks. It varies from continuous downpours to intermittent showers, often including intense rainstorms that pose significant threats to economic assets and property (Ding and Chan 2005; Ding et al. 2020).

In China, the term "Meiyu" refers to the rainy season occurring from mid-June to mid-July in the Yangtze-Huaihe River Basin (e.g., Tao and Chen 1987). In Japan, "Baiu" denotes the rainy period also from mid-June to mid-July, primarily affecting the Japanese archipelago (e.g., Ninomiya and Akiyama 1992). The Meiyu rain belt near eastern China generally follows almost a latitudinal direction, while in the Korean Peninsula and Japan, it extends toward east-northeast. Although the Meiyu-Baiu season occurs almost simultaneously in China and Japan, there are notable differences in the dynamical structure of the Meiyu-Baiu front (MBF) between the two regions (e.g., Sampe and Xie 2010). For example, Ding (2008) demonstrated that the regional differences are linked to large-scale circulation patterns, frontal structure, cloud and rain areas, mesoscale structure, and associated low-level jets. These differences are primarily attributed to the varying positions of the planetary-scale frontal zone and the seasonal evolution of the East Asian summer monsoon. Therefore, understanding these regional differences in the MBF system is crucial for accurate predictions of the regional rainfall and their future changes in specific areas.

Previous observational studies regarding the Meiyu-Baiu systems in China and Japan have primarily relied on case studies (e.g., Zheng et al. 2008; Liu et al. 2023) and composite methods (e.g., Zhang et al. 2006; Tong et al. 2022). For example, Tong et al. (2022) applied cluster analysis to examine the characteristics of the Meiyu belt in multiple datasets.

In this study, we utilized an MBF detection method based on previous research (Li et al. 2018; Li et al. 2021), aiming to investigate the atmospheric conditions along the front. The paper is structured as follows: Section 2 introduces the methodology for detecting the MBF and related precipitation. Section 3 presents the main results regarding precipitation and front activity. Section 4 provides the conclusion and discussion.

2. Data and methodology

2.1 Dataset

The daily products of precipitation and atmospheric variables in ECMWF Reanalysis v5 (ERA5) dataset (Hersbach et al. 2020) are utilized in the analysis. The horizontal resolution of the data is interpolated into 1° × 1° from the

Corresponding author: Sicheng He, Disaster Prevention Research Institute, Kyoto University, Gokasho, Uji, Kyoto 611-0011, Japan. E-mail: he_s@storm.dpri.kyoto-u.ac.jp.

original quarter-degree resolution. We examine the data from June to July during the time period from 1951 to 2010. To investigate the temporal change within the Meiyu/Baiu period the two-month period is divided into half-month intervals: early June (1–15 June), late June (16–30 June), early July (1–15 July), and late July (16–31 July).

2.2 Methodology

The study domain covers the area of 20°N–40°N and 105°E–145°E, encompassing the regions where Meiyu, Baiu, and Changma frequently occur. Previous studies mostly utilized equivalent potential temperature (θ_e) to define the locations of MBF. Based on the prior study of Li et al. (2018, 2021), we define the MBF as the band where the meridional gradient of θ_e at 850 hPa (θ_{e850}) is less than −0.04 K km^{-1}. The calculation procedure is as follows:

1. Calculate the θ_{e850} and its meridional gradient $\partial\theta_{e850}/\partial y$ for each grid point. Identify grid points where $\partial\theta_{e850}/\partial y$ is less than −0.04 K km^{-1}.
2. Determine the MBF center: For each longitude, compute the average latitude of grid points meeting this criterion, which is defined as the center latitude of the MBF. Isolated points that defined as a grid point where neither of its adjacent latitude points meets the criteria are excluded from this calculation to ensure that individual points meeting the criteria do not introduce bias in the positioning of the MBF.
3. Ensure continuity: Isolated MBF central points are further excluded, defined as points where neither adjacent longitude has valid MBF values, to ensure the MBF forms a continuous line.
4. Ensure sufficient length: For each day's MBF, the number of grid points representing its length should be no less than 70% of the entire region. This ensures that a sufficiently long MBF can be identified within the study domain.

Considering that Southeast China and Japanese region are regarded as key areas in East Asia for representing precipitation features during the Meiyu-Baiu season and exhibit maximum precipitation center, we chose these two subregions for regional analysis: Southeast China (SEC), ranging from 25°N to 35°N and 112°E to 122°E, and the Japanese region (JPN), ranging from 28°N to 38°N and 126°E to 136°E.

For better examining the atmospheric condition focusing the MBF, the vertical cross section along each MBF is calculated. The atmospheric conditions within a 5-degree latitude range north and south of each MBF were composited. The Meiyu-Baiu front related precipitation (MPR) is defined as the total precipitation (TPR) within a 2-degree latitude range north and south of each MBF, focusing on the meso-α scale precipitation related to the fronts.

The calculation is conducted on a daily basis. Supplementary Fig. S1 provides a daily example of MBF and MPR calculation.

For further analyzing the temperature and moisture component of MBF (Song et al. 2022), we computed the temperature (θ_e_T) and moisture (θ_e_M) components of θ_e as follows:

$$\theta_e \approx \left(T + \frac{L_v}{C_p} r\right)\left(\frac{p_0}{p}\right)^{R_d/C_p},$$

$$\theta_e\_T \approx T\left(\frac{p_0}{p}\right)^{R_d/C_p},$$

$$\theta_e\_M \approx \frac{L_v}{C_p} r\left(\frac{p_0}{p}\right)^{R_d/C_p},$$

where T, r, and p are temperature, water vapor mixing ratio, and pressure, respectively, and the constants L_v, C_p, p_0, and R_d are latent heat of vaporization (2.5 × 10^6 J kg^{-1}), specific heat of dry air at constant pressure (1005.7 J K^{-1} kg^{-1}), reference pressure (1000 hPa), and specific gas constant for air (287.04 J K^{-1} kg^{-1}).

3. Results

3.1 General features of MBF and MPR

The temporal variations in the position of the MBF every half-month during June and July are shown in Fig. 1. It is evident that the MBF gradually shifts northward with time. In early June, the MBF is situated over the Yangtze River Basin in southeastern China, while in the Japanese region, it is located to the south of Kyushu Island. By late June, the MBF shifts northward to the Huaihe River Basin in southeastern China and the Kyushu region in Japan. In July, the MBF continues its northward progression in southeastern China, while in Japan, it moves slowly in the northern part of Kyushu,

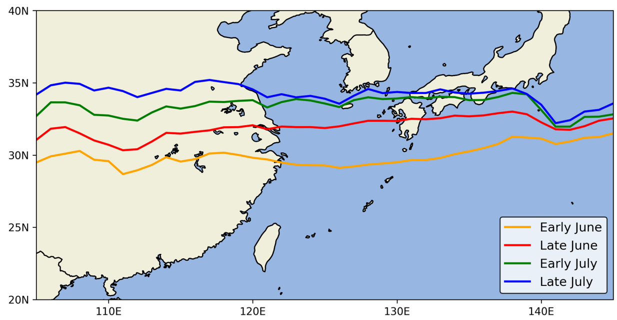

Fig. 1. The mean positions of the MBF averaged in each half-month period during June and July. The means are the time averages spanning from 1951 to 2010.

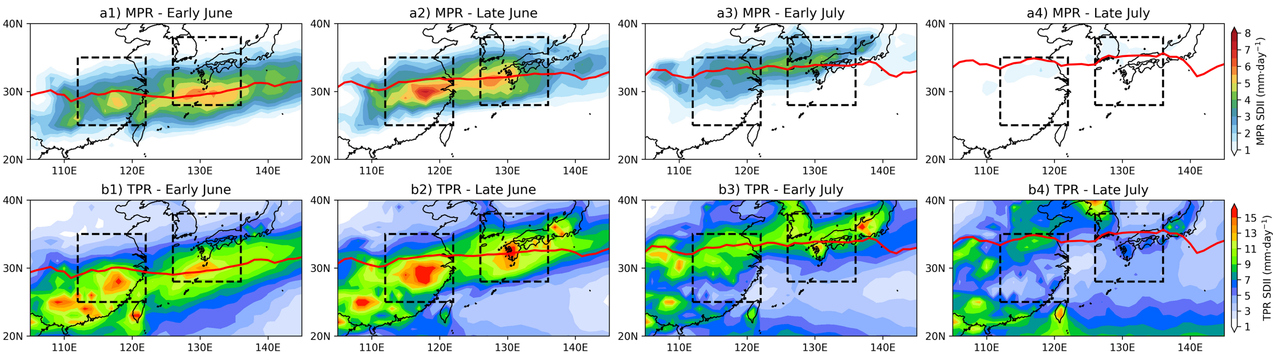

Fig. 2. Spatial distribution of daily precipitation intensity of Meiyu-Baiu front related precipitation (MPR, upper row) and total precipitation (TPR, lower row). Each column from left to right represents each half-month in June and July. The red line in each panel indicates the mean position of the MBF averaged during that specific time period.

Shikoku, and the southern part of Honshu Island. Near 140°E longitude, the MBF exhibits a southward extension in July, coinciding with its late June position. This may be attributed to a relatively limited sample of MBF observations in such easternmost locations, i.e., at the edge of the study area.

During each half-month period in the study area, total precipitation (TPR) and MBF-related precipitation (MPR) were investigated in Fig. 2. Generally, the spatial distributions of MPR and TPR look similar. MPR shows a close relationship with the position of the MBF, with precipitation areas migrating northward as the MBF propagates northward. It is noteworthy that in late July, the MBF is still discernible, yet there is a decrease in MPR. This is attributed to our definition of the MBF based on the meridional gradient of θ_e, thus maintaining a strong θ_e gradient while being unrelated to Meiyu precipitation. The spatial distribution of MPR in ERA5 was further compared with satellite observation data TRMM-3B42 within the overlapping time period of the two datasets (Fig. S2). A quantitative comparison reveals ERA5 generally captures observed spatial patterns but slightly overestimates precipitation intensity, particularly in June. These discrepancies highlight the need for caution when interpreting absolute precipitation magnitudes. However, the spatial-temporal patterns remain robust, making ERA5 suitable for comparative analysis.

By comparing the spatial distributions of TPR and MPR, it is found that from June to early July, approximately 50% of the TPR is contributed by MPR, which peaks in late June. While by late July, the MPR (MBF) has shifted northward to around 35°N, whereas the precipitation center of TPR appears near 20°N, indicating a transition into another rainy season when precipitation is likely driven more by tropical cyclones and local-scale thunderstorms (Ding et al. 2007). In June, MPR exhibits two precipitation centers, located in southeastern China and the Japanese region, which are also reflected in the spatial distribution of TPR.

3.2 Regional and temporal variability of front activity

In the following, we examine the atmospheric conditions associated with the front in the two key regions, based on half-month periods. The features of circulation patterns and moisture transport in the northern and southern parts of the MBF in each half-month period in the JPN and SEC regions are indicated. Specifically, the zonal, meridional, and vertical motion fields as well as the horizontal moisture fluxes are investigated. Then, the temperature and moisture contributions of the θ_e fields are demonstrated to diagnose the stability conditions for the occurrence of MBF.

The East Asian subtropical westerly jet (EASWJ) is a crucial component of the East Asian summer monsoon system. Its seasonal northward jump and southward retreat are significantly associated with the precipitation anomalies in East Asia (Zhou et al. 2005; Zhou et al. 2009). Figure 3 illustrates the vertical cross section of zonal wind and zonal moisture flux within 5 degrees latitudes centered at the MBF. In both regions, the zonal wind exhibits a strong jet at the 200-hPa level on the northern side of the MBF. The jet is the strongest in early June and gradually weakens until late July. In June, the jet is stronger in the JPN region than in SEC, while in July, it becomes weaker in JPN than in SEC. These features are consistent with the previous study by Endo et al. (2021). The zonal wind in the lower troposphere on the southern side of the MBF in the JPN region consistently remains slightly stronger than that in the SEC region. A significant amount of westerly moisture flux is seen in the lower troposphere on the southern side of MBF both in JPN and SEC, which is the strongest in late June. The JPN region exhibits a stronger westerly moisture flux in the lower atmosphere compared to the SEC region during this period. The features are also evident in the spatial distribution of atmospheric conditions (Fig. S3). The EASWJ is positioned on the north side of the mean location of the MBF, while the moisture transport is concentrated on the south side of the MBF.

Meridional components of horizontal winds and moisture fluxes are demonstrated in Fig. 4. Southerly flux near the surface is observed on the southern side of the MBF in both regions and during each time period. In SEC, the maximum

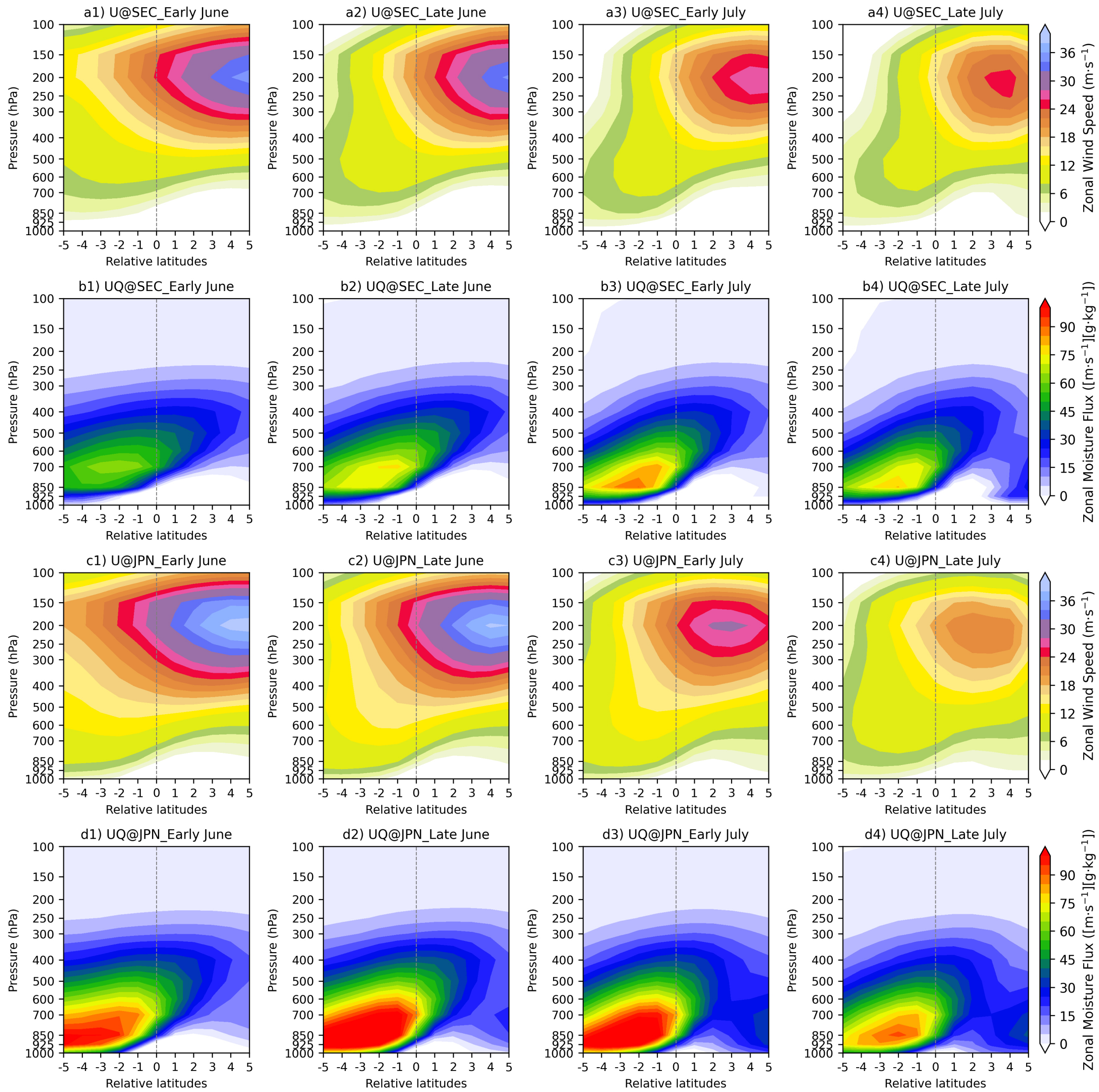

Fig. 3. Vertical cross section of zonal wind speed and zonal moisture flux within 5 degrees latitudes, positive (negative) denoting the north (the south), centered at the MBF over SEC (top two rows) and JPN (bottom two rows) for each half-month period. The columns from left to right represent from early June to late July. The dash line represents the center of MBF. The panels on the first and third rows indicate the cross sections for the zonal winds, while those on the second and 4th rows for the zonal moisture flux.

southerly moisture flux occurs from late June to early July, while in JPN, it peaks in early and late June.

Regarding the vertical velocity (Fig. 5), upward motion is seen on the southern side of MBF with the maximum value at 500 hPa. The upward motion weakens with time in both regions. The maximum upward motion appears in late June in SEC, while in early June in JPN.

Here we examined the temperature and moisture components of θ_e. Figure 6 shows the vertical cross section of the differences of these components as well as θ_e between SEC and JPN. The actual values in each region are shown in Figs. S4 and S5. By comparing the anomalies in SEC against JPN, the two regions indicate contrasting features. It is evident that the SEC region indicates a higher value of θ_e_M on the southern side of MBF, leading to a larger meridional gradient of humidity at around MBF. On the other hand, because of the higher value of θ_e_T on the northern side of MBF, the temperature meridional gradient is smaller in SEC than in JPN. Therefore, the meridional gradient of θ_e is primarily contributed by the meridional gradient of moisture in SEC while contributed by the temperature gradient in JPN. The sub-seasonal march demonstrated here occurs in relation to the northward propagation of the East Asian summer monsoon. As shown in the seasonal march of the western Pacific subtropical high (WPSH) in Fig. S3, from early June to late July, the position of the MBF accompanies the northward propagation of the WPSH. From late June to early July, the WPSH extends westward, resulting in an increased moisture gradient in the SEC region.

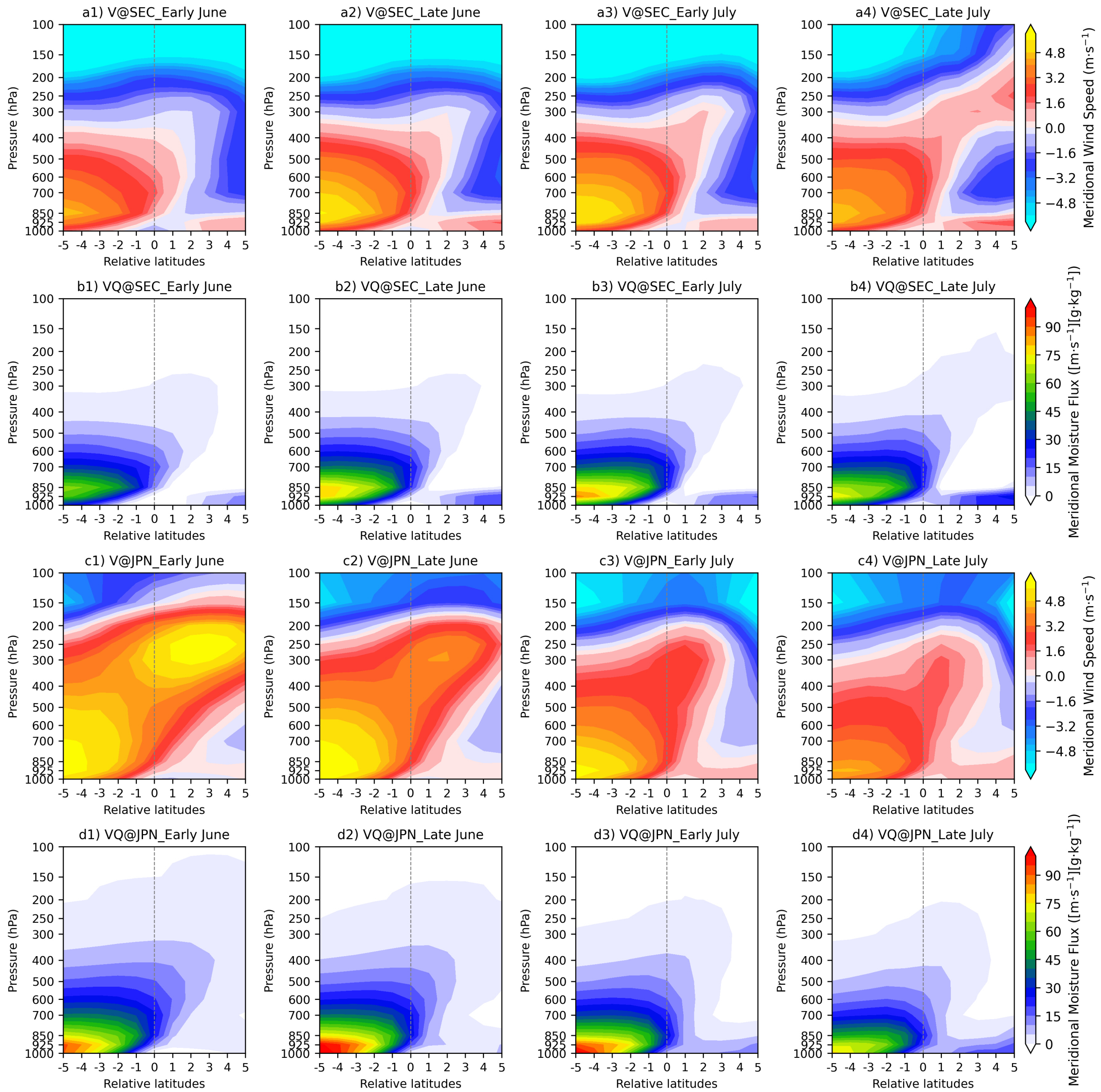

Fig. 4. As in Fig. 3, but for meridional wind speed and moisture flux.

4. Conclusion and discussion

Based on ERA5 reanalysis data and a method defining the Meiyu-Baiu front (MBF) based on equivalent potential temperature, we analyzed the precipitation and atmospheric conditions during the East Asian monsoon season. By analyzing a long time period climatology, we compared the difference in Meiyu-Baiu front in Southeast China (SEC) region and Japan (JPN) region, respectively. We found that the MBF exhibits a clear northward movement in the SEC region from early June to late July, while in the JPN region it moves northward from early June to mid-July and then becomes slower in late July. The Meiyu-Baiu precipitation shows a good correlation with the position of the MBF from early June to mid-July, locating two major centers in both the SEC and JPN regions.

The atmospheric conditions associated with the MBF exhibit both regional and temporal variability. On the southern side of the MBF, the JPN exhibits a stronger zonal and meridional moisture flux than the SEC region. While in terms of the thermodynamic features, the SEC region shows a stronger meridional humidity gradient and smaller meridional temperature gradient compared to the JPN. Notably, in the JPN region, intense MPR is concentrated along the frontal zone, whereas in the SEC region, peak precipitation occurs south of the front. Further analysis is needed to demonstrate the precipitation pattern differences related to the front activities in the two regions.

This study employs high-resolution ERA5 data to analyze the Meiyu-Baiu front (MBF) precipitation and atmospheric environment over a 60-year period at a sub-seasonal scale (half-month intervals), comparing the differences between Southeast China and the Japan region. The significance and innovation of this research lie in its comprehensive

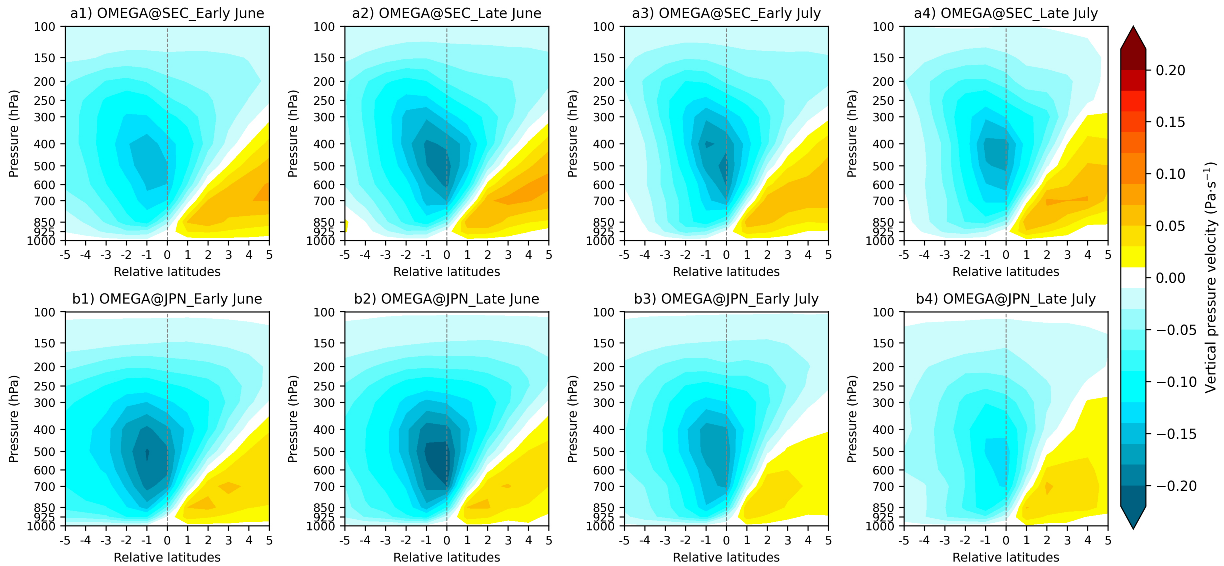

Fig. 5. As in Fig. 3, but for vertical pressure velocity.

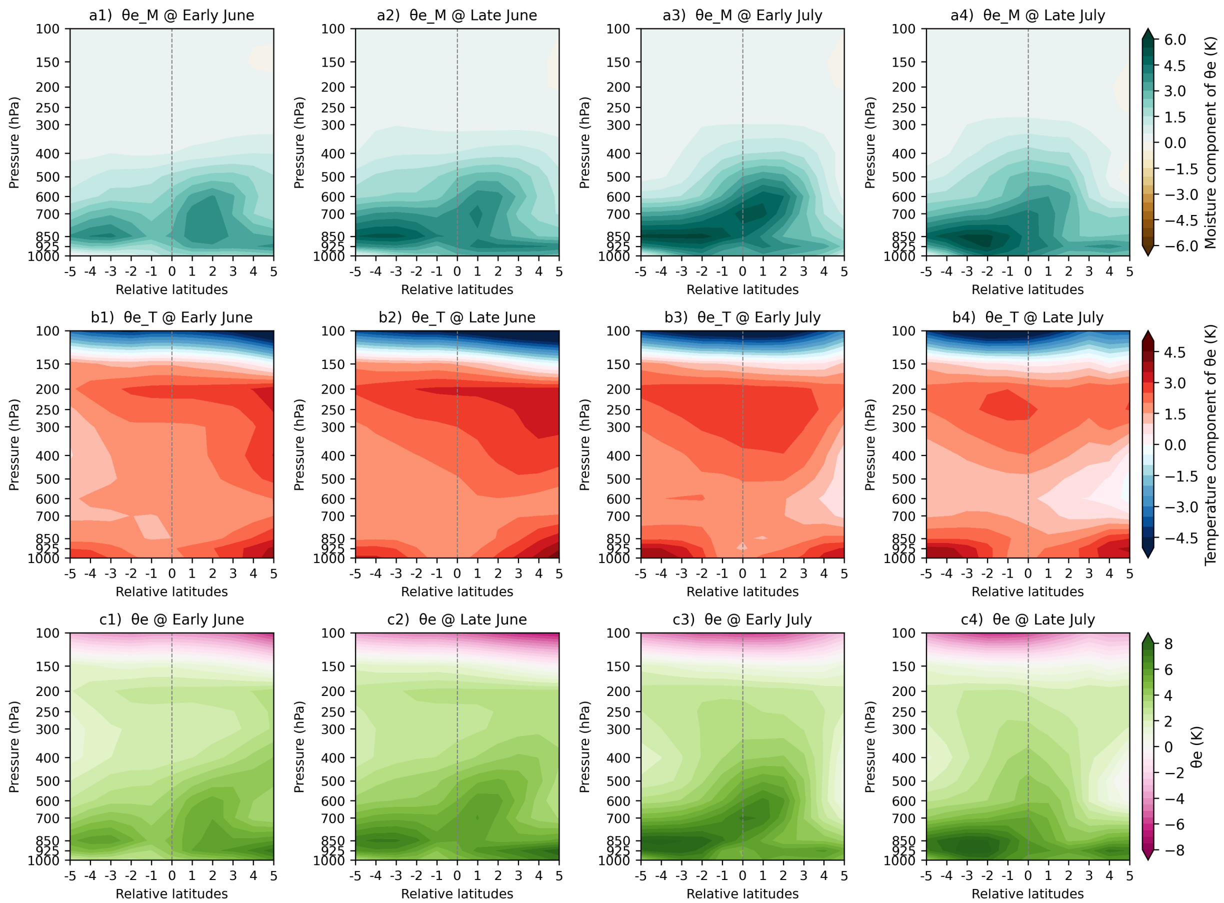

Fig. 6. Vertical cross section of moisture component (θ_e_M, top row), temperature component (θ_e_T, middle row) and θ_e (bottom row) within 5 degrees latitude south and north of the MBF, showing regional difference between SEC minus JPN. The columns from left to right represent half month period from early June to late July.

examination of regional variability in MBF dynamics over an extended timespan, offering new insights into the sub-seasonal characteristics of precipitation patterns and atmospheric conditions across different geographical areas. These findings provide valuable input for improving climate models in simulating front activity and front-related precipitation, serving as a foundation for more accurate forecasting across various timeframes and regions in the future. The identified different structures of MBF in SEC and JPN can serve as a useful observational metric for model evaluations and improvement.

Acknowledgements

The comments from two anonymous reviewers are greatly acknowledged to improve the quality of the manuscript. This study is supported by the Japan Society for the Promotion of Science (JSPS) Scientific Research 24H00369 and also by the advanced studies of climate change projection (SENTAN) Grant Number JPMXD0722678534 from the Ministry of Education, Culture, Sports, Science and Technology (MEXT) of Japan.

Edited by: C.-C. Wang

Supplements

The Supplementary Material include supplementary figures providing methodological details, and extended analyses supporting the main findings of this study.

References

Ding, Y., 1992: Summer monsoon rainfalls in China. *J. Meteor. Soc. Japan*, **70**, 373–396, doi:10.2151/jmsj1965.70.1B_373.

Ding, Y., P. Liang, Y. Liu, and Y. Zhang, 2020: Multiscale variability of Meiyu and its prediction: A new review. *J. Geophys. Res.: Atmos.*, **125**, e2019JD031496, doi:10.1029/2019JD031496.

Ding, Y., Z. Wang, and Y. Sun, 2008: Inter-decadal variation of the summer precipitation in East China and its association with decreasing Asian summer monsoon. Part I: Observed evidences. *Int. J. Climatol.*, **28**, 1139–1161, doi:10.1002/joc.1615.

Ding, Y., and J. C. L. Chan, 2005: The East Asian summer monsoon: An overview. *Meteor. Atmos. Phys.*, **89**, 117–142, doi:10.1007/s00703-005-0125-z.

Endo, H., A. Kitoh, R. Mizuta, and T. Ose, 2021: Different future changes between early and late summer monsoon precipitation in East Asia. *J. Meteor. Soc. Japan*, **99**, 1501–1524, doi:10.2151/jmsj.2021-073.

Hersbach, H., B. Bell, P. Berrisford, and co-authors, 2020: The ERA5 global reanalysis. *Quart. J. Roy. Meteor. Soc.*, **146**, 1999–2049, doi:10.1002/qj.3803.

Li, Y., Y. Deng, S. Yang, and H. Zhang, 2018: Multi-scale temporospatial variability of the East Asian Meiyu-Baiu fronts: Characterization with a suite of new objective indices. *Climate Dyn.*, **51**, 1659–1670, doi:10.1007/s00382-017-3975-4.

Li, Y., N.-C. Lau, C.-Y. Tam, H.-N. Cheung, Y. Deng, and H. Zhang, 2021: Projected changes in the characteristics of the East Asian summer monsoonal front and their impacts on the regional precipitation. *Climate Dyn.*, **56**, 4013–4026, doi:10.1007/s00382-021-05687-y.

Liu, C., C. Hu, S. Yang, T. Lian, C. Zhang, L. Lin, and F. Cai, 2023: Extreme Mei-yu in 2020: Characteristics, causes, predictability and perspectives. *Earth-Sci. Rev.*, **246**, 104597, doi:10.1016/j.earscirev.2023.104597.

Ninomiya, K., and T. Akiyama, 1992: Multi-scale features of Baiu, the summer monsoon over Japan and the East Asia. *J. Meteor. Soc. Japan*, **70**, 467–495, doi:10.2151/jmsj1965.70.1B_467.

Sampe, T., and S.-P. Xie, 2010: Large-scale dynamics of the Meiyu-Baiu rainband: Environmental forcing by the westerly jet. *J. Climate*, **23**, 113–134, doi:10.1175/2009JCLI3128.1.

Song, F., G. J. Zhang, V. Ramanathan, and L. R. Leung, 2022: Trends in surface equivalent potential temperature: A more comprehensive metric for global warming and weather extremes. *Proc. Natl. Acad. Sci. U.S.A. (PNAS)*, **119**, e2117832119, doi:10.1073/pnas.2117832119.

Tao, S. Y., and L. X. Chen, 1987: A review of recent research on the East Asian summer monsoon in China. *Monsoon Meteorology*. C.-P. Chang, and T. N. Krishnamurti, Eds., Oxford University Press, 60–92.

Tong, M., Z. Zheng, and Q. Fu, 2022: Evaluation of East Asian Meiyu from CMIP6/AMIP simulations. *Climate Dyn.*, **59**, 2429–2444, doi:10.1007/s00382-022-06218-z.

Zhang, C.-Z., H. Uyeda, H. Yamada, B. Geng, and Y. Ni, 2006: Characteristics of mesoscale convective systems over the east part of continental China during the Meiyu from 2001 to 2003. *J. Meteor. Soc. Japan*, **84**, 763–782, doi:10.2151/jmsj.84.763.

Zheng, Y., J. Chen, G. Ge, and P. Zhu, 2008: Typical structure, variety, and multi-scale characteristics of Meiyu front. *J. Meteor. Res.*, **22**, 187–201.

Zhou, T.-J., and R.-C. Yu, 2005: Atmospheric water vapor transport associated with typical anomalous summer rainfall patterns in China. *J. Geophys. Res.*, **110**, D08104, doi:10.1029/2004JD005413.

Zhou, T., D. Gong, J. Li, and B. Li, 2009: Detecting and understanding the multi-decadal variability of the East Asian summer monsoon recent progress and state of affairs. *Meteor. Z.*, **18**, 455–467, doi:10.1127/0941-2948/2009/0396.